Measurement of $\sigma_{\Lambda_b^0}/\sigma_{\bar{B}^0} \times \mathcal{B}\left(\Lambda_b^0 \rightarrow \Lambda_c^+\pi^-\right)/\mathcal{B}\left(\bar{B}^0 \rightarrow D^+\pi^-\right)$ in $p\bar{p}$ Collisions at $\sqrt{s} = 1.96$ TeV

A. Abulencia,[23] D. Acosta,[17] J. Adelman,[13] T. Affolder,[10] T. Akimoto,[53] M.G. Albrow,[16] D. Ambrose,[16] S. Amerio,[42] D. Amidei,[33] A. Anastassov,[50] K. Anikeev,[16] A. Annovi,[44] J. Antos,[1] M. Aoki,[53] G. Apollinari,[16] J.-F. Arguin,[32] T. Arisawa,[55] A. Artikov,[14] W. Ashmanskas,[16] A. Attal,[8] F. Azfar,[41] P. Azzi-Bacchetta,[42] P. Azzurri,[44] N. Bacchetta,[42] H. Bachacou,[28] W. Badgett,[16] A. Barbaro-Galtieri,[28] V.E. Barnes,[46] B.A. Barnett,[24] S. Baroiant,[7] V. Bartsch,[30] G. Bauer,[31] F. Bedeschi,[44] S. Behari,[24] S. Belforte,[52] G. Bellettini,[44] J. Bellinger,[57] A. Belloni,[31] E. Ben-Haim,[16] D. Benjamin,[15] A. Beretvas,[16] J. Beringer,[28] T. Berry,[29] A. Bhatti,[48] M. Binkley,[16] D. Bisello,[42] M. Bishai,[16] R. E. Blair,[2] C. Blocker,[6] K. Bloom,[33] B. Blumenfeld,[24] A. Bocci,[48] A. Bodek,[47] V. Boisvert,[47] G. Bolla,[46] A. Bolshov,[31] D. Bortoletto,[46] J. Boudreau,[45] S. Bourov,[16] A. Boveia,[10] B. Brau,[10] C. Bromberg,[34] E. Brubaker,[13] J. Budagov,[14] H.S. Budd,[47] S. Budd,[23] K. Burkett,[16] G. Busetto,[42] P. Bussey,[20] K. L. Byrum,[2] S. Cabrera,[15] M. Campanelli,[19] M. Campbell,[33] F. Canelli,[8] A. Canepa,[46] D. Carlsmith,[57] R. Carosi,[44] S. Carron,[15] M. Casarsa,[52] A. Castro,[5] P. Catastini,[44] D. Cauz,[52] M. Cavalli-Sforza,[3] A. Cerri,[28] L. Cerrito,[41] S.H. Chang,[27] J. Chapman,[33] Y.C. Chen,[1] M. Chertok,[7] G. Chiarelli,[44] G. Chlachidze,[14] F. Chlebana,[16] I. Cho,[27] K. Cho,[27] D. Chokheli,[14] J.P. Chou,[21] P.H. Chu,[23] S.H. Chuang,[57] K. Chung,[12] W.H. Chung,[57] Y.S. Chung,[47] M. Ciljak,[44] C.I. Ciobanu,[23] M.A. Ciocci,[44] A. Clark,[19] D. Clark,[6] M. Coca,[15] A. Connolly,[28] M. E. Convery,[48] J. Conway,[7] B. Cooper,[30] K. Copic,[33] M. Cordelli,[18] G. Cortiana,[42] A. Cruz,[17] J. Cuevas,[11] R. Culbertson,[16] D. Cyr,[57] S. DaRonco,[42] S. D'Auria,[20] M. D'onofrio,[19] D. Dagenhart,[6] P. de Barbaro,[47] S. De Cecco,[49] A. Deisher,[28] G. De Lentdecker,[47] M. Dell'Orso,[44] S. Demers,[47] L. Demortier,[48] J. Deng,[15] M. Deninno,[5] D. De Pedis,[49] P.F. Derwent,[16] C. Dionisi,[49] J. Dittmann,[4] P. DiTuro,[50] C. Dörr,[25] A. Dominguez,[28] S. Donati,[44] M. Donega,[19] P. Dong,[8] J. Donini,[42] T. Dorigo,[42] S. Dube,[50] K. Ebina,[55] J. Efron,[38] J. Ehlers,[19] R. Erbacher,[7] D. Errede,[23] S. Errede,[23] R. Eusebi,[47] H.C. Fang,[28] S. Farrington,[29] I. Fedorko,[44] W.T. Fedorko,[13] R.G. Feild,[58] M. Feindt,[25] J.P. Fernandez,[46] R. Field,[17] G. Flanagan,[34] L.R. Flores-Castillo,[45] A. Foland,[21] S. Forrester,[7] G.W. Foster,[16] M. Franklin,[21] J.C. Freeman,[28] Y. Fujii,[26] I. Furic,[13] A. Gajjar,[29] M. Gallinaro,[48] J. Galyardt,[12] J.E. Garcia,[44] M. Garcia Sciverez,[28] A.F. Garfinkel,[46] C. Gay,[58] H. Gerberich,[23] E. Gerchtein,[12] D. Gerdes,[33] S. Giagu,[49] P. Giannetti,[44] A. Gibson,[28] K. Gibson,[12] C. Ginsburg,[16] K. Giolo,[46] M. Giordani,[52] M. Giunta,[44] G. Giurgiu,[12] V. Glagolev,[14] D. Glenzinski,[16] M. Gold,[36] N. Goldschmidt,[33] J. Goldstein,[41] G. Gomez,[11] G. Gomez-Ceballos,[11] M. Goncharov,[51] O. González,[46] I. Gorelov,[36] A.T. Goshaw,[15] Y. Gotra,[45] K. Goulianos,[48] A. Gresele,[42] M. Griffiths,[29] S. Grinstein,[21] C. Grosso-Pilcher,[13] U. Grundler,[23] J. Guimaraes da Costa,[21] C. Haber,[28] S.R. Hahn,[16] K. Hahn,[43] E. Halkiadakis,[47] A. Hamilton,[32] B-Y. Han,[47] R. Handler,[57] F. Happacher,[18] K. Hara,[53] M. Hare,[54] S. Harper,[41] R.F. Harr,[56] R.M. Harris,[16] K. Hatakeyama,[48] J. Hauser,[8] C. Hays,[15] H. Hayward,[29] A. Heijboer,[43] B. Heinemann,[29] J. Heinrich,[43] M. Hennecke,[25] M. Herndon,[57] J. Heuser,[25] D. Hidas,[15] C.S. Hill,[10] D. Hirschbuehl,[25] A. Hocker,[16] A. Holloway,[21] S. Hou,[1] M. Houlden,[29] S.-C. Hsu,[9] B.T. Huffman,[41] R.E. Hughes,[38] J. Huston,[34] K. Ikado,[55] J. Incandela,[10] G. Introzzi,[44] M. Iori,[49] Y. Ishizawa,[53] A. Ivanov,[7] B. Iyutin,[31] E. James,[16] D. Jang,[50] B. Jayatilaka,[33] D. Jeans,[49] H. Jensen,[16] E.J. Jeon,[27] M. Jones,[46] K.K. Joo,[27] S.Y. Jun,[12] T.R. Junk,[23] T. Kamon,[51] J. Kang,[33] M. Karagoz-Unel,[37] P.E. Karchin,[56] Y. Kato,[40] Y. Kemp,[25] R. Kephart,[16] U. Kerzel,[25] V. Khotilovich,[51] B. Kilminster,[38] D.H. Kim,[27] H.S. Kim,[27] J.E. Kim,[27] M.J. Kim,[12] M.S. Kim,[27] S.B. Kim,[27] S.H. Kim,[53] Y.K. Kim,[13] M. Kirby,[15] L. Kirsch,[6] S. Klimenko,[17] M. Klute,[31] B. Knuteson,[31] B.R. Ko,[15] H. Kobayashi,[53] K. Kondo,[55] D.J. Kong,[27] J. Konigsberg,[17] A. Korytov,[17] A.V. Kotwal,[15] A. Kovalev,[43] J. Kraus,[23] I. Kravchenko,[31] M. Kreps,[25] A. Kreymer,[16] J. Kroll,[43] N. Krumnack,[4] M. Kruse,[15] V. Krutelyov,[51] S. E. Kuhlmann,[2] Y. Kusakabe,[55] S. Kwang,[13] A.T. Laasanen,[46] S. Lai,[32] S. Lami,[48] S. Lami,[48] S. Lammel,[16] M. Lancaster,[30] R. L. Lander,[7] K. Lannon,[38] A. Lath,[50] G. Latino,[44] I. Lazzizzera,[42] Y. Le,[24] C. Lecci,[25] T. LeCompte,[2] J. Lee,[47] J. Lee,[47] S.W. Lee,[51] R. Lefèvre,[3] N. Leonardo,[31] S. Leone,[44] S. Levy,[13] J.D. Lewis,[16] K. Li,[58] C. Lin,[58] C.S. Lin,[16] M. Lindgren,[16] E. Lipeles,[9] T.M. Liss,[23] A. Lister,[19] D.O. Litvintsev,[16] T. Liu,[16] Y. Liu,[19] N.S. Lockyer,[43] A.Loginov,[35] M. Loreti,[42] P. Loverre,[49] R.-S. Lu,[1] D. Lucchesi,[42] P. Lujan,[28] P. Lukens,[16] G. Lungu,[17] L. Lyons,[41] J. Lys,[28] R. Lysak,[1] E. Lytken,[46] P. Mack,[25] D. MacQueen,[32] R. Madrak,[16] K. Maeshima,[16] P. Maksimovic,[24] G. Manca,[29] F. Margaroli,[5] R. Marginean,[16] C. Marino,[23] A. Martin,[58] M. Martin,[24] V. Martin,[37] M. Martínez,[3] T. Maruyama,[53] H. Matsunaga,[53] M.E. Mattson,[56] R. Mazini,[32] P. Mazzanti,[5] K.S. McFarland,[47] D. McGivern,[30] P. McIntyre,[51] P. McNamara,[50] R. McNulty,[29] A. Mehta,[29] S. Menzemer,[31] A. Menzione,[44] P. Merkel,[46] C. Mesropian,[48] A. Messina,[49] M. von der Mey,[8] T. Miao,[16] N. Miladinovic,[6] J. Miles,[31] R. Miller,[34] J.S. Miller,[33] C. Mills,[10] M. Milnik,[25] R. Miquel,[28] S. Miscetti,[18] G. Mitselmakher,[17] A. Miyamoto,[26] N. Moggi,[5] B. Mohr,[8] R. Moore,[16]

M. Morello,[44] P. Movilla Fernandez,[28] J. Mülmenstädt,[28] A. Mukherjee,[16] M. Mulhearn,[31] Th. Muller,[25] R. Mumford,[24] P. Murat,[16] J. Nachtman,[16] S. Nahn,[58] I. Nakano,[39] A. Napier,[54] D. Naumov,[36] V. Necula,[17] C. Neu,[43] M.S. Neubauer,[9] J. Nielsen,[28] T. Nigmanov,[45] L. Nodulman,[2] O. Norniella,[3] T. Ogawa,[55] S.H. Oh,[15] Y.D. Oh,[27] T. Okusawa,[40] R. Oldeman,[29] R. Orava,[22] K. Osterberg,[22] C. Pagliarone,[44] E. Palencia,[11] R. Paoletti,[44] V. Papadimitriou,[16] A. Papikonomou,[25] A.A. Paramonov,[13] B. Parks,[38] S. Pashapour,[32] J. Patrick,[16] G. Pauletta,[52] M. Paulini,[12] C. Paus,[31] D. E. Pellett,[7] A. Penzo,[52] T.J. Phillips,[15] G. Piacentino,[44] J. Piedra,[11] K. Pitts,[23] C. Plager,[8] L. Pondrom,[57] G. Pope,[45] X. Portell,[3] O. Poukhov,[14] N. Pounder,[41] F. Prakoshyn,[14] A. Pronko,[16] J. Proudfoot,[2] F. Ptohos,[18] G. Punzi,[44] J. Pursley,[24] J. Rademacker,[41] A. Rahaman,[45] A. Rakitin,[31] S. Rappoccio,[21] F. Ratnikov,[50] B. Reisert,[16] V. Rekovic,[36] N. van Remortel,[22] P. Renton,[41] M. Rescigno,[49] S. Richter,[25] F. Rimondi,[5] K. Rinnert,[25] L. Ristori,[44] W.J. Robertson,[15] A. Robson,[20] T. Rodrigo,[11] E. Rogers,[23] S. Rolli,[54] R. Roser,[16] M. Rossi,[52] R. Rossin,[17] C. Rott,[46] A. Ruiz,[11] J. Russ,[12] V. Rusu,[13] D. Ryan,[54] H. Saarikko,[22] S. Sabik,[32] A. Safonov,[7] W.K. Sakumoto,[47] G. Salamanna,[49] O. Salto,[3] D. Saltzberg,[8] C. Sanchez,[3] L. Santi,[52] S. Sarkar,[49] K. Sato,[53] P. Savard,[32] A. Savoy-Navarro,[16] T. Scheidle,[25] P. Schlabach,[16] E.E. Schmidt,[16] M.P. Schmidt,[58] M. Schmitt,[37] T. Schwarz,[33] L. Scodellaro,[11] A.L. Scott,[10] A. Scribano,[44] F. Scuri,[44] A. Sedov,[46] S. Seidel,[36] Y. Seiya,[40] A. Semenov,[14] F. Semeria,[5] L. Sexton-Kennedy,[16] I. Sfiligoi,[18] M.D. Shapiro,[28] T. Shears,[29] P.F. Shepard,[45] D. Sherman,[21] M. Shimojima,[53] M. Shochet,[13] Y. Shon,[57] I.Shreyber,[35] A. Sidoti,[44] P. Sinervo,[32] A. Sisakyan,[14] J. Sjolin,[41] A. Skiba,[25] A.J. Slaughter,[16] K. Sliwa,[54] D. Smirnov,[36] J. R. Smith,[7] F.D. Snider,[16] R. Snihur,[32] M. Soderberg,[33] A. Soha,[7] S. Somalwar,[50] V. Sorin,[34] J. Spalding,[16] F. Spinella,[44] P. Squillacioti,[44] M. Stanitzki,[58] A. Staveris-Polykalas,[44] R. St. Denis,[20] B. Stelzer,[8] O. Stelzer-Chilton,[32] D. Stentz,[37] J. Strologas,[36] D. Stuart,[10] J.S. Suh,[27] A. Sukhanov,[17] K. Sumorok,[31] H. Sun,[54] T. Suzuki,[53] A. Taffard,[23] R. Tafirout,[32] R. Takashima,[39] Y. Takeuchi,[53] K. Takikawa,[53] M. Tanaka,[2] R. Tanaka,[39] M. Tecchio,[33] P.K. Teng,[1] K. Terashi,[48] S. Tether,[31] J. Thom,[16] A.S. Thompson,[20] E. Thomson,[43] P. Tipton,[47] V. Tiwari,[12] S. Tkaczyk,[16] D. Toback,[51] K. Tollefson,[34] T. Tomura,[53] D. Tonelli,[44] M. Tönnesmann,[34] S. Torre,[44] D. Torretta,[16] S. Tourneur,[16] W. Trischuk,[32] J. Tseng,[31] R. Tsuchiya,[55] S. Tsuno,[39] N. Turini,[44] F. Ukegawa,[53] T. Unverhau,[20] S. Uozumi,[53] D. Usynin,[43] L. Vacavant,[28] A. Vaiciulis,[47] S. Vallecorsa,[19] A. Varganov,[33] E. Vataga,[36] G. Velev,[16] G. Veramendi,[23] V. Veszpremi,[46] T. Vickey,[23] R. Vidal,[16] I. Vila,[11] R. Vilar,[11] I. Vollrath,[32] I. Volobouev,[28] F. Würthwein,[9] P. Wagner,[51] R. G. Wagner,[2] R.L. Wagner,[16] W. Wagner,[25] R. Wallny,[8] T. Walter,[25] Z. Wan,[50] M.J. Wang,[1] S.M. Wang,[17] A. Warburton,[32] B. Ward,[20] S. Waschke,[20] D. Waters,[30] T. Watts,[50] M. Weber,[28] W.C. Wester III,[16] B. Whitehouse,[54] D. Whiteson,[43] A. B. Wicklund,[2] E. Wicklund,[16] H.H. Williams,[43] P. Wilson,[16] B.L. Winer,[38] P. Wittich,[43] S. Wolbers,[16] C. Wolfe,[13] S. Worm,[50] T. Wright,[33] X. Wu,[19] S.M. Wynne,[29] A. Yagil,[16] K. Yamamoto,[40] J. Yamaoka,[50] Y. Yamashita.,[39] C. Yang,[58] U.K. Yang,[13] W.M. Yao,[28] G.P. Yeh,[16] J. Yoh,[16] K. Yorita,[13] T. Yoshida,[40] I. Yu,[27] S.S. Yu,[43] J.C. Yun,[16] L. Zanello,[49] A. Zanetti,[52] I. Zaw,[21] F. Zetti,[44] X. Zhang,[23] J. Zhou,[50] and S. Zucchelli[5]

(CDF Collaboration)

[1]*Institute of Physics, Academia Sinica, Taipei, Taiwan 11529, Republic of China*
[2]*Argonne National Laboratory, Argonne, Illinois 60439*
[3]*Institut de Fisica d'Altes Energies, Universitat Autonoma de Barcelona, E-08193, Bellaterra (Barcelona), Spain*
[4]*Baylor University, Waco, Texas 76798*
[5]*Istituto Nazionale di Fisica Nucleare, University of Bologna, I-40127 Bologna, Italy*
[6]*Brandeis University, Waltham, Massachusetts 02254*
[7]*University of California, Davis, Davis, California 95616*
[8]*University of California, Los Angeles, Los Angeles, California 90024*
[9]*University of California, San Diego, La Jolla, California 92093*
[10]*University of California, Santa Barbara, Santa Barbara, California 93106*
[11]*Instituto de Fisica de Cantabria, CSIC-University of Cantabria, 39005 Santander, Spain*
[12]*Carnegie Mellon University, Pittsburgh, PA 15213*
[13]*Enrico Fermi Institute, University of Chicago, Chicago, Illinois 60637*
[14]*Joint Institute for Nuclear Research, RU-141980 Dubna, Russia*
[15]*Duke University, Durham, North Carolina 27708*
[16]*Fermi National Accelerator Laboratory, Batavia, Illinois 60510*
[17]*University of Florida, Gainesville, Florida 32611*
[18]*Laboratori Nazionali di Frascati, Istituto Nazionale di Fisica Nucleare, I-00044 Frascati, Italy*
[19]*University of Geneva, CH-1211 Geneva 4, Switzerland*
[20]*Glasgow University, Glasgow G12 8QQ, United Kingdom*
[21]*Harvard University, Cambridge, Massachusetts 02138*
[22]*Division of High Energy Physics, Department of Physics, University of Helsinki and Helsinki Institute of Physics, FIN-00014, Helsinki, Finland*

[23] University of Illinois, Urbana, Illinois 61801
[24] The Johns Hopkins University, Baltimore, Maryland 21218
[25] Institut für Experimentelle Kernphysik, Universität Karlsruhe, 76128 Karlsruhe, Germany
[26] High Energy Accelerator Research Organization (KEK), Tsukuba, Ibaraki 305, Japan
[27] Center for High Energy Physics: Kyungpook National University, Taegu 702-701; Seoul National University, Seoul 151-742; and SungKyunKwan University, Suwon 440-746; Korea
[28] Ernest Orlando Lawrence Berkeley National Laboratory, Berkeley, California 94720
[29] University of Liverpool, Liverpool L69 7ZE, United Kingdom
[30] University College London, London WC1E 6BT, United Kingdom
[31] Massachusetts Institute of Technology, Cambridge, Massachusetts 02139
[32] Institute of Particle Physics: McGill University, Montréal, Canada H3A 2T8; and University of Toronto, Toronto, Canada M5S 1A7
[33] University of Michigan, Ann Arbor, Michigan 48109
[34] Michigan State University, East Lansing, Michigan 48824
[35] Institution for Theoretical and Experimental Physics, ITEP, Moscow 117259, Russia
[36] University of New Mexico, Albuquerque, New Mexico 87131
[37] Northwestern University, Evanston, Illinois 60208
[38] The Ohio State University, Columbus, Ohio 43210
[39] Okayama University, Okayama 700-8530, Japan
[40] Osaka City University, Osaka 588, Japan
[41] University of Oxford, Oxford OX1 3RH, United Kingdom
[42] University of Padova, Istituto Nazionale di Fisica Nucleare, Sezione di Padova-Trento, I-35131 Padova, Italy
[43] University of Pennsylvania, Philadelphia, Pennsylvania 19104
[44] Istituto Nazionale di Fisica Nucleare Pisa, Universities of Pisa, Siena and Scuola Normale Superiore, I-56127 Pisa, Italy
[45] University of Pittsburgh, Pittsburgh, Pennsylvania 15260
[46] Purdue University, West Lafayette, Indiana 47907
[47] University of Rochester, Rochester, New York 14627
[48] The Rockefeller University, New York, New York 10021
[49] Istituto Nazionale di Fisica Nucleare, Sezione di Roma 1, University di Roma "La Sapienza," I-00185 Roma, Italy
[50] Rutgers University, Piscataway, New Jersey 08855
[51] Texas A&M University, College Station, Texas 77843
[52] Istituto Nazionale di Fisica Nucleare, University of Trieste/ Udine, Italy
[53] University of Tsukuba, Tsukuba, Ibaraki 305, Japan
[54] Tufts University, Medford, Massachusetts 02155
[55] Waseda University, Tokyo 169, Japan
[56] Wayne State University, Detroit, Michigan 48201
[57] University of Wisconsin, Madison, Wisconsin 53706
[58] Yale University, New Haven, Connecticut 06520

(Dated: December 22, 2005)

We present the first observation of the baryon decay $\Lambda_b^0 \to \Lambda_c^+\pi^-$ followed by $\Lambda_c^+ \to pK^-\pi^+$ in 106 pb^{-1} $p\bar{p}$ collisions at $\sqrt{s} = 1.96$ TeV in the CDF experiment. In order to reduce systematic error, the measured rate for Λ_b^0 decay is normalized to the kinematically similar meson decay $\bar{B}^0 \to D^+\pi^-$ followed by $D^+ \to \pi^+K^-\pi^+$. We report the ratio of production cross sections (σ) times the ratio of branching fractions ($\mathcal{B}$) for the momentum region integrated above $p_T > 6$ GeV/c and pseudorapidity range $|\eta| < 1.3$: $\sigma(p\bar{p} \to \Lambda_b^0 X)/\sigma(p\bar{p} \to \bar{B}^0 X) \times \mathcal{B}(\Lambda_b^0 \to \Lambda_c^+\pi^-)/\mathcal{B}(\bar{B}^0 \to D^+\pi^-) = 0.82 \pm 0.08$ (stat) ± 0.11 (syst) ± 0.22 ($\mathcal{B}(\Lambda_c^+ \to pK^-\pi^+)$).

PACS numbers: 14.20.Mr, 13.30.Eg, 14.65.Fy

Weak decays of baryons containing b quarks are a good laboratory for testing the Heavy Quark Effective Theory (HQET) [1]. The Λ_b^0 baryon is the ground state of the udb quark system, and, in the heavy quark limit, the light degrees of freedom are in the state of zero total angular momentum [2]. Fully hadronic $b \to c\bar{u}d$ transitions are more complicated in baryons than in mesons because there are diagrams which are not present in the decays of the latter. Various extensions of HQET have been used to evaluate the $\Lambda_b^0 \to \Lambda_c^+\pi^-$ decay rate [3], but the predictions vary over a large range. However, in Soft Collinear Effective Theory (SCET) [4], all tree-level amplitudes can be properly evaluated, resulting in an explicit prediction for the ratio of branching fractions $\mathcal{B}(\Lambda_b^0 \to \Lambda_c^+\pi^-)/\mathcal{B}(\bar{B}^0 \to D^+\pi^-) \approx 1.7$ [5]. The decays of Λ_b^0 are also interesting because they may provide a means to determine CKM matrix elements with different systematic uncertainties than the determinations from the decays of B mesons [6].

This is the first reconstruction of a hadronic decay of a b baryon at a hadron collider that does not use a J/ψ in the final state. In addition, our sample has more than an order of magnitude more events than any previous sample of fully reconstructed Λ_b^0 decays, and, for the same luminosity, is about five times larger than a sample of $\Lambda_b \rightarrow J/\psi\Lambda$ decays. Since b baryons are not produced at the B factories operating at the $\Upsilon(4S)$ resonance, studying them comprises a unique facet of the B physics program at Collider Detector at Fermilab (CDF II) [7]. In particular, a large sample of fully reconstructed Λ_b^0 decays would allow CDF to study other properties of b baryons, *e.g.*, to measure the lifetime of Λ_b^0, and also to search for decays of heavier b baryons such as $\Sigma_b^\pm \rightarrow \Lambda_b^0\pi^\pm$.

This paper presents a measurement of a ratio of Λ_b^0 and $\bar{B}^0$ branching fractions multiplied by the ratio of production cross-sections,

$$R \equiv \frac{\sigma(p\bar{p} \rightarrow \Lambda_b^0 X)}{\sigma(p\bar{p} \rightarrow \bar{B}^0 X)} \times \frac{\mathcal{B}(\Lambda_b^0 \rightarrow \Lambda_c^+\pi^-)}{\mathcal{B}(\bar{B}^0 \rightarrow D^+\pi^-)}, \qquad (1)$$

where the σ quantities are the cross-sections for Λ_b^0 and $\bar{B}^0$ production in the pseudorapidity range $|\eta| < 1.3$ with momentum in the transverse plane, p_T, above 6 GeV/c [8].

The quantity R compares the branching fractions of the topologically similar, fully reconstructed decays $\Lambda_b^0 \rightarrow \Lambda_c^+\pi^-$ and $\bar{B}^0 \rightarrow D^+\pi^-$, where the charmed hadrons decay via similar three-body channels $\Lambda_c^+ \rightarrow pK^-\pi^+$ and $D^+ \rightarrow \pi^+K^-\pi^+$ [9]. To extract a branching ratio, a good understanding of the absolute reconstruction efficiency is needed. However, to obtain R only the ratio of the reconstruction efficiencies of two topologically and kinematically similar decay modes is evaluated, significantly reducing the systematic errors on the measured quantity.

The upgraded CDF II detector is well-suited for the detailed study of weak decays of heavy baryons. In particular, the advent of the Silicon Vertex Trigger (SVT) [10], which uses precise position measurements to select events containing weakly decaying heavy hadrons, allows CDF II to collect many hadronic decay modes of heavy baryons for the first time. This measurement is performed using a 106 pb^{-1} sample of $p\bar{p}$ collisions collected by CDF II between February 2002 and June 2003. This data sample corresponds to $\sim 10^9$ b hadron decays produced in the central detector region. A full description of the CDF II detector can be found elsewhere [7]. The detector components pertinent to this analysis are the silicon microstrip vertex detector (SVX II) [11], the drift-chamber central tracker (COT) [12] and a three-tiered trigger system (Levels 1, 2, and 3). The five double-sided layers of the SVX II used in this analysis provide up to 10 position measurements. Of these, up to five are in the r-ϕ [8] plane (each precise to about 15 μm), three are longitudinal, and two are small-angle-stereo. The ϕ strips are parallel to the z-axis, longitudinal strips are inclined at 90°, and the small-angle-stereo strips are inclined at 1.2°. The SVX II spans the radii between 2.5 and 10.6 cm, and covers the pseudorapidity range $|\eta| < 2$. The COT has 96 measurement layers between the radii of 40 and 137 cm. These are organized into alternating axial and small-angle-stereo (2°) super-layers. The COT has a smaller pseudorapidity coverage ($|\eta| < 1.3$) than the SVX II. Both tracking detectors are immersed in a 1.41 T magnetic field parallel to the z axis.

This analysis in particular relies on the SVT, which operates as a part of the Level 2 trigger system. The trigger makes it possible to select events at a rate of ~ 100 Hz from the ~ 1 MHz interaction rate. The components of the three level trigger system pertinent to this measurement are the Extremely Fast Tracker (XFT) at Level 1 and the SVT at Level 2. The XFT uses four axial super-layers of the COT to find tracks with $p_T > 1.5$ GeV/c. The SVT combines the XFT measurement with $r-\phi$ hits from the SVX II detector. The track finding is performed using a large look-up table of hit patterns. The found track candidates are fitted for curvature, angle projected onto the transverse plane and impact-parameter [13]. The impact-parameter measurement allows the selection of long-lived particles in the trigger decision.

The signal (Λ_b^0) and normalization ($\bar{B}^0$) events are collected using the same trigger. At Level 1, two tracks must satisfy $p_T > 2.0$ GeV/c, a scalar sum of transverse momenta $p_{T1} + p_{T2} > 5.5$ GeV/c, and an angular separation projected onto the transverse plane of $\Delta\phi < 135°$. At Level 2 the transverse momentum cuts are repeated, and it is required that each track has impact parameter $d_0 > 120$ μm, with an angular separation between the tracks projected onto the transverse plane of ($2° < \Delta\phi < 90°$). Finally, the distance evaluated in the transverse plane from the primary vertex to the two-track intersection point must be greater than 200 μm.

Additional criteria are imposed on the triggered sample in order to reject as many background events as possible while keeping most of the signal. To reconstruct $\Lambda_b^0 \rightarrow \Lambda_c^+\pi^-$, minimum acceptable COT and SVX hit requirements are imposed, and all valid four track combinations are considered. The p_T of the proton candidate from the Λ_c^+ and the π^- candidate from the Λ_b^0 must be greater than 2.0 GeV/c, which strongly favors these particles to be the two which caused the event to pass the trigger. The p_T of the proton candidate must be larger than the p_T of the π^+ candidate from the Λ_c^+. The p_T of the Λ_b^0 and Λ_c^+ candidates must be greater than 7.5 GeV/c and 4.5 GeV/c, respectively. In Equation (1), $\sigma_{\Lambda_b^0}$ and $\sigma_{\bar{B}^0}$ are defined for $p_T > 6$ GeV/c. The events in the data sample must satisfy $p_T > 7.5$ GeV/c, and the difference is accounted for by using the Monte Carlo simulation based on the p_T distributions of both Λ_b^0 and $\bar{B}^0$ measured in data [14].

Each of the unstable particles (Λ_b^0, $\bar{B}^0$, Λ_c^+, and D^+) is reconstructed by considering all valid combinations of tracks and requiring them to satisfy the decay hypothesis. The charmed hadrons Λ_c^+ and D^+ are reconstructed first: each triplet of tracks that satisfies the selection criteria (detailed below) is constrained to pass through the same point, called the decay vertex. The decay vertex is determined by varying the track parameters of the stable daughters within their uncertainties to minimize the χ^2. The $\Lambda_c^+(D^+)$ candidate is then combined with a fourth track to form a $\Lambda_b^0(\bar{B}^0)$ candidate. The full topology of the decay is then imposed in another kinematic fit, resulting in a simultaneous measurement of the Λ_b^0 $(\bar{B}^0)$ and Λ_c^+ (D^+) vertices.

Using these measurements, the reconstructed invariant mass of the Λ_c^+ must be between 2.269 GeV$/c^2$ and 2.301 GeV$/c^2$. Other selection criteria rely on L_{xy}, the projection onto the x-y (transverse) plane of the decay length measured from the production vertex to the decay point; the production vertex is estimated by the position of the beamline averaged over each run calculated for the z coordinate of the secondary vertex. A product of the proper decay time and the speed of light, ct, is also used. It is derived from L_{xy}: $ct = (\vec{L}_{xy} \cdot \hat{p}_T)(mc/p_T)$, where $\vec{L}_{xy}$ is the decay vector of Λ_b^0 $(\bar{B}^0)$ projected onto the x-y plane, p_T is the transverse momentum, $\hat{p}_T$ is the unit vector in the direction of the transverse momentum, and m is the world average mass of the Λ_b^0 $(\bar{B}^0)$. In order to suppress the combinatorial background from the interaction point, we impose $ct(\Lambda_b^0) > 225$ μm (compared to the b baryon mean decay length of 368 ± 24 μm [15]). Calculated relative to the Λ_b^0 decay point, $ct(\Lambda_c^+)$ must be $ct(\Lambda_c^+) > -65$ μm. For a true Λ_c^+, a small negative ct may arise due to resolution effects; on the other hand, the $ct(\Lambda_c^+)$ of combinatorial background candidates may have large negative values. The distance of closest approach in the transverse plane of the trajectory of the Λ_b^0 candidate to the primary vertex must be less than 85 μm. The χ^2_{xy} of the Λ_b^0 and Λ_c^+ kinematic fits are required to be less than 30 and 20 respectively, where χ^2_{xy} is a χ^2-like goodness-of-fit quantity using only the track parameters in the transverse plane.

The normalization mode ($\bar{B}^0 \to D^+\pi^-$) is reconstructed using selection criteria identical to those of the signal mode, except for a different invariant mass requirement for the D^+ candidate and no analogy to the $p_T(p) > p_T(\pi^+)$ cut. The D^+ candidate invariant mass must be between 1.848 GeV$/c^2$ and 1.888 GeV$/c^2$. The distributions of the invariant mass of $\Lambda_b^0 \to \Lambda_c^+\pi^-$ and $\bar{B}^0 \to D^+\pi^-$ candidates are shown in Figures 1 and 2, respectively.

Figure 1 shows the binned likelihood fit to the invariant mass distribution of Λ_b^0 candidates. The large Gaussian peak at 5.6 GeV$/c^2$ is the signal. The dash-dotted curve corresponds to the exponential combinatorial background. This component is constrained by the data in the invariant mass region above the Λ_b^0 mass. The small asymmetric peak at 5.5 GeV$/c^2$ (solid line) corresponds to contributions from fully reconstructed B-meson decays resulting in a final state with four tracks, where at least one track is misidentified. This shape is obtained using a full detector simulation of these modes. It is consistent with the shape of $\bar{B}^0 \to D^+\pi^-$ candidates found in the Λ_b^0 sample. The dotted and dashed curves correspond to all the other B-meson and Λ_b^0 backgrounds, respectively. These shapes are determined from a large parametric Monte Carlo sample which includes all known decays of B^+, B^0, and B_s and Λ_b^0 hadrons. Finally, there is a very small Gaussian distribution (not shown) from the Cabibbo-suppressed mode $\Lambda_b^0 \to \Lambda_c^+ K^-$ (fixed to an expected 8% of the signal yield [16]). The total distribution is $F_{\rm tot} = G_{\rm signal} + E_{\rm comb} + F_{\rm four-track} + F_{\rm other-B} + F_{{\rm other}-\Lambda_b^0} + G_{\Lambda_c^+K^-}$, where G indicates a Gaussian distribution, E indicates an exponential, and F indicates a

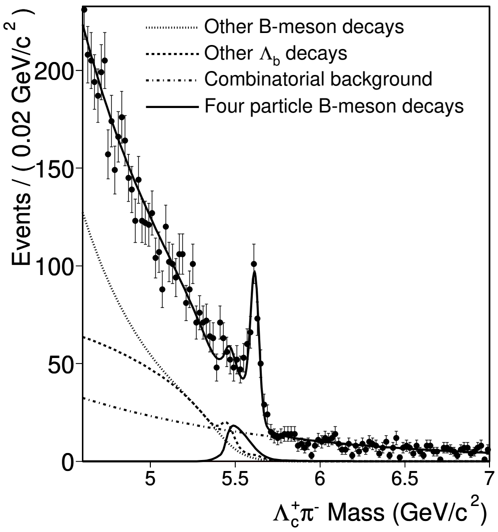

FIG. 1: $\Lambda_b^0 \to \Lambda_c^+\pi^-$ yield with binned likelihood mass fit. The background shapes are defined in the text.

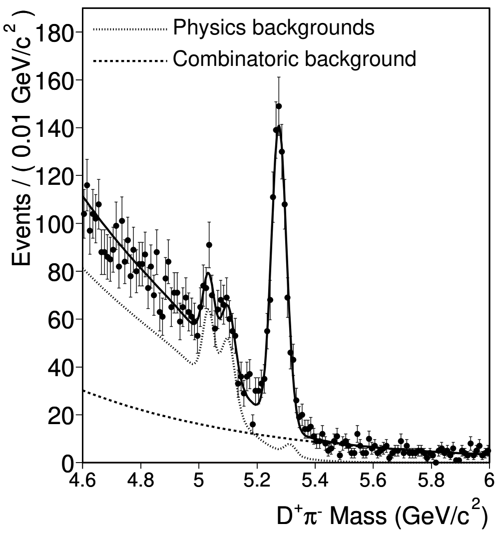

FIG. 2: $\bar{B}^0 \to D^+\pi^-$ yield with binned likelihood fit. The background shapes are defined in the text.

more complicated functional form.

In the fit, the width of Λ_b^0 signal is fixed to 26.4 MeV$/c^2$, obtained by scaling the $\bar{B}^0$ width in data by the ratio of widths from the Monte Carlo simulation. The relative contribution of each background type in the fit is guided by two constraints: the first describes the normalization of $F_{\text{four-track}}$ relative to $F_{\text{other-B}}$ (*i.e.*, $N_{\text{four-track}}/N_{\text{other-B}}$), where N is number of events; the second describes the normalization of $F_{\text{other}-\Lambda_b^0}$ relative to $(F_{\text{other-B}} + F_{\text{four-track}})$, (*i.e.*, $N_{\text{other }\Lambda_b^0}/(N_{\text{four-track}} + N_{\text{other-B}})$). The value of each constraint is inferred from the relative abundance of the background types in the large parametric Monte Carlo sample. The value of the $(N_{\text{four-track}}/N_{\text{other-B}})$ constraint is checked by reconstructing the $\bar{B}^0 \to D^+\pi^-$ mode among $\Lambda_c^+\pi^-$ candidates from the region of the invariant mass corresponding to the Λ_b^0 signal. The total χ^2 of this fit is 80.6 for 88 degrees of freedom, corresponding to the fit probability of 70%.

Figure 2 shows the mass fit for the $D^+\pi^-$ candidates. The large Gaussian peak at 5.27 GeV$/c^2$ is the $\bar{B}^0$ signal. The dashed curve corresponds to the exponential combinatorial background. The dotted curve corresponds to the background from decays of other b hadrons. The total χ^2 of this fit is 70.9 for 94 degrees of freedom, corresponding to the fit probability of 96%.

The quantity R defined in equation (1) is calculated from the signal yield according to

$$R = \frac{N_{\Lambda_b^0}}{N_{\bar{B}^0}} \times \frac{\mathcal{B}(D^+ \to \pi^+K^-\pi^+)}{\mathcal{B}(\Lambda_c^+ \to pK^-\pi^+)} \times \frac{\epsilon(\bar{B}^0)}{\epsilon(\Lambda_b^0)}, \qquad (2)$$

where the first factor is the ratio of observed signal yields, the second factor is the ratio of the daughter branching fractions [15], and the third factor is the ratio of reconstruction efficiencies calculated from the Monte Carlo. The signal yields are $N_{\Lambda_b^0} = 214 \pm 19$ and $N_{\bar{B}^0} = 790 \pm 32$ respectively. Each reconstruction efficiency is defined for the $\Lambda_b^0(\bar{B}^0)$ with $p_T > 6$ GeV$/c$ and $|\eta| < 1.3$. The exact configuration of the CDF II detector varied over the course of collecting the data used in the analysis. However, the ratio of reconstruction efficiencies is stable within statistical errors across the different periods of running, with the average value $\epsilon(\bar{B}^0)/\epsilon(\Lambda_b^0) = 1.65 \pm 0.03$. From Equation (2) we thus obtain $R = 0.82 \pm 0.08(\text{stat})$.

The systematic uncertainty on the measurement of R is dominated by the error on $\mathcal{B}(\Lambda_c^+ \to pK^-\pi^+)$, yielding a relative error of 27% [15]. Since this uncertainty is independent of our measurement, it is quoted separately. Other sources of systematic uncertainty are the imperfect knowledge of the Λ_b^0 lifetime ($^{+5}_{-4}$%), the production p_T spectra of both Λ_b^0 (7.6%) and $\bar{B}^0$ (4%), the Λ_b^0 polarization (7%), and the Λ_c^+ resonant substructure (1%). The uncertainty due to the finite size of the Monte Carlo samples is 1.9%. The uncertainty due to the difference between the proton and π^+ trigger efficiency is 0.6%. The systematic uncertainties due to the background shapes in the invariant mass fits are 4.3% for the Λ_b^0 and 0.9% for the $\bar{B}^0$. These uncertainties arise from the lack of detailed knowledge of a variety of branching fractions contributing to background shapes that are obtained from the Monte Carlo simulation and fixed in the fit. To evaluate the uncertainty due to these shapes, the branching fractions of the largest decay modes contributing to each of the shapes were varied simultaneously in the simulation, and the shapes were reevaluated. Uncertainties on the mass resolutions of both Λ_b^0 and $\bar{B}^0$, which are also fixed in the mass fits, contribute 2.8% and 1.8%, respectively. Finally, the contribution of the $\Lambda_b^0 \to \Lambda_c^+K^-$ shape is varied by a factor of 2, contributing 1.6% to the systematic error. The total systematic error excluding the uncertainty on $\mathcal{B}(\Lambda_c^+ \to pK^-\pi^+)$ is 13.5%.

A direct comparison with a theoretical prediction of $R_{BR} \equiv \mathcal{B}(\Lambda_b^0 \to \Lambda_c^+\pi^-)/\mathcal{B}(\bar{B}^0 \to D^{(*)+}\pi^-) \approx 1.7$ [5] can be performed if one assumes that $\sigma(\Lambda_b)$ and $\sigma(B^0)$ have the same dependence on p_T, and then use f_{baryon}/f_d from high-p_T measurements. From Ref. [15] we obtain $f_{\text{baryon}}/f_d = 0.25 \pm 0.04$, which yields $R_{BR} \approx 3.3 \pm 1.2$, in agreement with [5].

In summary, we have observed the decay $\Lambda_b^0 \to \Lambda_c^+\pi^-$ for the first time, and measured $R = 0.82 \pm 0.08(\text{stat}) \pm 0.11\ (\text{syst}) \pm 0.22\ (\mathcal{B}_{\Lambda_c^+})$. The overall error is dominated by the large uncertainty on $\mathcal{B}(\Lambda_c^+ \to pK^-\pi^+)$. The $\Lambda_b^0 \to \Lambda_c^+\pi^-$ sample is the largest b-baryon sample in existence, and, once augmented by new data, can be used for a variety of other Λ_b measurements, including its lifetime and production properties.

We thank the Fermilab staff and the technical staffs of the participating institutions for their vital contributions. This work was supported by the U.S. Department of Energy and National Science Foundation; the Italian Istituto Nazionale di Fisica Nucleare; the Ministry of Education, Culture, Sports, Science and Technology of Japan; the Natural Sciences and Engineering Research Council of Canada; the National Science Council of the Republic of China; the Swiss National Science Foundation; the A.P. Sloan Foundation; the Bundesministerium für Bildung und Forschung, Germany; the Korean Science and Engineering Foundation and the Korean Research Foundation; the Particle Physics and Astronomy Research Council and the Royal Society, UK; the Russian Foundation for Basic Research; the Comisión Interministerial de Ciencia y Tecnología, Spain; in part by the European Community's Human Potential Programme under contract HPRN-CT-2002-00292; and the Academy of Finland.

[1] For a review, see A. F. Falk, "Introduction to hadronic B physics," Chapter 2 of 'The BaBar Physics Book: Physics at an Asymmetric B Factory', arXiv:hep-ph/9812217,

and references therein.

[2] A. F. Falk and M. Neubert, Phys. Rev. D **47**, 2982 (1993).

[3] X. H. Guo, Mod. Phys. Lett. A **13**, 2265 (1998).

[4] C. W. Bauer, S. Fleming and M. E. Luke, Phys. Rev. D **63**, 014006 (2001); C. W. Bauer, S. Fleming, D. Pirjol and I. W. Stewart, Phys. Rev. D **63**, 114020 (2001); C. W. Bauer and I. W. Stewart, Phys. Lett. B **516**, 134 (2001); C. W. Bauer, D. Pirjol and I. W. Stewart, Phys. Rev. D **65**, 054022 (2002).

[5] A. K. Leibovich, Z. Ligeti, I. W. Stewart and M. B. Wise, Phys. Lett. B **586**, 337 (2004).

[6] I. Dunietz, Z. Phys. C **56**, 129 (1992).

[7] D. Acosta *et al.* Phys. Rev. D **71**, 032001 (2005)

[8] CDF II uses a cylindrical coordinate system with the z-axis along the nominal beam-line. The transverse plane (x, y) is perpendicular to the z-axis. Azimuthal angle, ϕ, is measured from the x-axis. Polar angle, θ, is measured from the z-axis. Pseudorapidity is defined as $\eta \equiv \tanh^{-1}(\cos\theta)$. Transverse momentum, p_T, is the component of the particle's momentum projected onto the transverse plane.

[9] Inclusion of the respective charge conjugate modes is assumed throughout this paper. Specifically, $\bar{\Lambda}_b^0 \to \Lambda_c^- \pi^+$, $B^0 \to D^- \pi^+$, $\Lambda_c^- \to \bar{p} K^+ \pi^-$, and $D^- \to \pi^- K^+ \pi^-$.

[10] W. Ashmanskas *et al.*, Nucl. Instrum. Meth. A **518**, 532 (2004).

[11] A. Sill *et al.*, Nucl. Instrum. Meth. A **447**, 1 (2000).

[12] A. Affolder *et al.*, Nucl. Instrum. Meth. A **526**, 249 (2004).

[13] The curvature of a particle track is inversely proportional to the transverse momentum (p_T). The impact-parameter of a particle track is defined as the distance of closest approach of the particle track to the primary vertex in the transverse plane.

[14] S. Yu, PhD thesis, University of Pennsylvania, 2005 (unpublished). [arXiv:hep-ex/0504059].

[15] S. Eidelman *et al.*, Phys. Lett. B **592**, 1 (2004).

[16] This choice is motivated by K. Abe *et al.*, Phys. Rev. Lett. **87**, 111801 (2001), however we assign a large systematic error to it.